




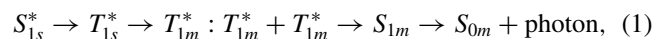
Kinetics of near-infrared-to-visible upconversion in rubrene: An initial excitation of tripletsPushpendra Kumar ^{*}*Max-Planck Institute of Polymer Research, Ackermannweg 10, 55128 Mainz, Germany*Durga Prasad Kandel  and Rajendra Adhikari *Department of Physics, Kathmandu University, Box:6250, Kavre, Nepal*Ahibur Rahaman ^{*}*Department of Organic Chemistry, Arrhenius Laboratory Stockholm University, Svante Arrhenius vag 16C, 10691 Stockholm, Sweden*Khadga J. Karki [†]*Guangdong Technion-Israel Institute of Technology, 241 Daxue Road, Shantou, Guangdong Province 515603, People's Republic of China* (Received 22 July 2021; revised 10 October 2021; accepted 14 October 2021; published 28 October 2021)

Upconversion (UC) in a molecular system is a process in which excitons produced by a multiple absorption of low-energy photons at long wavelengths undergo fusion to produce high energy excitons that consequently recombine to emit anti-Stokes shifted photons. Molecular systems for UC typically require a sensitizer. However, recent experiments show that UC in rubrene occurs even without the presence of the sensitizer. In this system, intermediate states are assumed to absorb photons at near-infrared wavelengths, which either absorb additional photons to populate the emissive singlet state or undergo fusion to generate triplets. The triplets can again undergo fusion to populate the excited singlet state. The final emission is around 600 nm. These models have been tested against the intensity dependence of the UC emission. Here, we have measured the kinetics of UC in rubrene by using intensity modulated photoexcitation at 800 nm to better understand the underlying mechanism. The models of UC that have been proposed so far do not agree with our measurements. Our results show that the yield of UC lags behind excitation significantly, indicating that triplet states are directly excited from the ground state, and their fusion, which depends on the population, becomes prominent after a certain build up time. While the intermediate states could form dynamically after the UC has been initiated and enhance the process, further sensitive absorption measurements are necessary to understand the role of the intermediate states in the process. Our results are important in finding new routes to enhance UC in pristine organic semiconductors for applications in photovoltaics, lasers, bioimaging, optical devices, and lighting.

DOI: [10.1103/PhysRevB.104.L140308](https://doi.org/10.1103/PhysRevB.104.L140308)**I. INTRODUCTION**

Upconversion (UC) in molecular systems proceeds via the fusion of two triplet excitations. As the direct excitation of triplet states from a typical singlet ground state is spin forbidden, it is common to use sensitizers for the initial excitation. The overall mechanism involves excitation of the sensitizer, which undergoes intersystem crossing to populate the triplet states followed by the energy transfer to the triplet states of the molecules of interest. Diffusion mediated fusion of two such molecular excitations leads to a simultaneous excitation of a high lying singlet state in one of the molecules and de-excitation in the other [1–4]. This process is also commonly known as triplet-triplet annihilation (TTA) [5,6]. The molecules that have been excited to the singlet state undergo radiative recombination emitting photons with higher energies

compared to the photons initially absorbed by the sensitizer. A simple scheme of the UC in a typical molecular system is given in Eq.(1):



where S_{1s} and T_{1s} are the first singlet and triplet states of the sensitizer, S_{1m} and T_{1m} are the first singlet and triplet states of the chromophore and S_{0m} is the corresponding ground state. One of the advantages of TTA based UC is the availability of a huge array of molecular systems that can upconvert photons from ultraviolet (UV) to near-infrared (NIR) wavelength [7]. UC has been observed in different classes of chromophores including anthracene [3], tetracene [4], pyrene, and perylene [8] and diimide based derivatives [9]. UC in these systems have found numerous applications in lasers, [10] optical devices, [11,12] bioimaging, [13–15] photovoltaics, and lighting [16–18].

While the initial excitation of the singlet state of the sensitizer is essential for the efficient absorption of low energy photons in a typical molecular system for UC, recent measurements have shown an exception in rubrene where the

^{*}Chemical Physics, Department of Chemistry, Lund University, Box 120, SE-221 00 Lund, Sweden.

[†]khadga.karki@gtiit.edu.cn

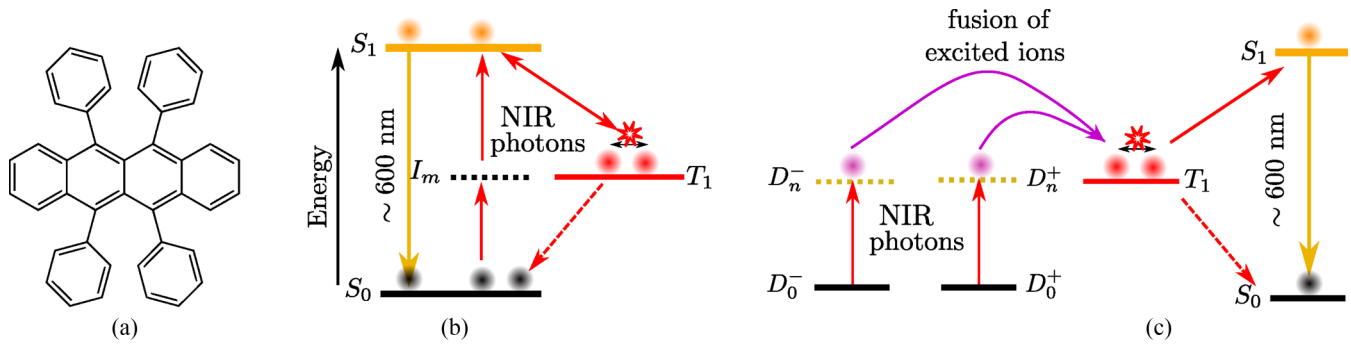


FIG. 1. (a) Molecular structure of rubrene. (b) Model of up-conversion in rubrene where the intermediate state enhances the absorption of multiple photon. (c) Alternative model of upconversion where the initial excitation is of the residual ions in the crystals. The excited ions fuse to excite triplets which then undergoes to triplet-triplet annihilation to produce the emissive singlet excitation.

process occurs efficiently even without an extrinsic sensitizer [19–21].

Rubrene is one of the best performing material among all the benchmark organic semiconductors [22–24]. It is a p-type semiconductor and derivative of tetracene having four pendant phenyl groups attached to the central rings [Fig. 1(a)]. It has been extensively studied due to the exceptional high hole mobilities and chemical stability [24–26]. Rubrene is also a prototypical organic semiconductor that exhibits efficient fission of a singlet excitation into a pair of triplets and the reverse process of fusion of triplets to a singlet by TTA. It is known that the triplet state T_1 in rubrene is at 1.14 eV above its singlet ground state, whereas the optical energy gap of rubrene, corresponding to the transition to the S_1 state, is 2.23 eV [27,28]. This condition makes TTA favorable.

So far, two models have been proposed to explain the process [19–21]. The energy diagrams and the processes involved in the models are shown in Figs. 1(b) and 1(c). Both the models assume the presence of an intermediate state that facilitates UC. The first model by Liu *et al.* [19] proposes the intermediate state to be a virtual state that is present only during the interaction with the photons while the model by Cruz *et al.* [20] assumes it to be a weakly resonant state [see Fig. 1(b)]. In this model, the UC occurs by a sequential excitation. The model by Beimborn *et al.* [21] assumes that the trapped charges, denoted by D_0 and D_n in Fig. 1(c) (both cations and anions), absorb the low energy photons and become mobile. As they diffuse through the crystal, occasionally oppositely charged ions meet and fuse to produce the excited triplet excitons, which then undergo TTA. The different models take into account some aspects of the experimental observations, such as nonlinear dependence of the UC on the intensity of incident photons and the excitation spectrum. However, these models fail to explain the kinetics of the process, which we report here. Our results are explained by a simplified three state model in which the UC is initiated by the very weak excitation of the triplet state from the ground state. The TTA populates the emissive singlet state that relaxes to the ground state by emitting upconverted photons. Although our results do not exclude the pathways that include intermediate states, such states clearly are not present in the initial build up of the population in the triplet state. We outline further experiments to understand how the intermediate states could be formed, and their contribution to the UC in rubrene.

II. MATERIALS AND METHODS

For our measurements, rubrene (5,6,11,12-Tetraphenyl-naphthacene) as a red colored powder was purchased from Sigma Aldrich and used without further purification. Fig. 2(a) shows a schematic of the setup used to detect UC emission by intensity modulation. It is based on a similar setup for spectroscopy using phase modulation [29–33]. A CW Ti-Sapphire

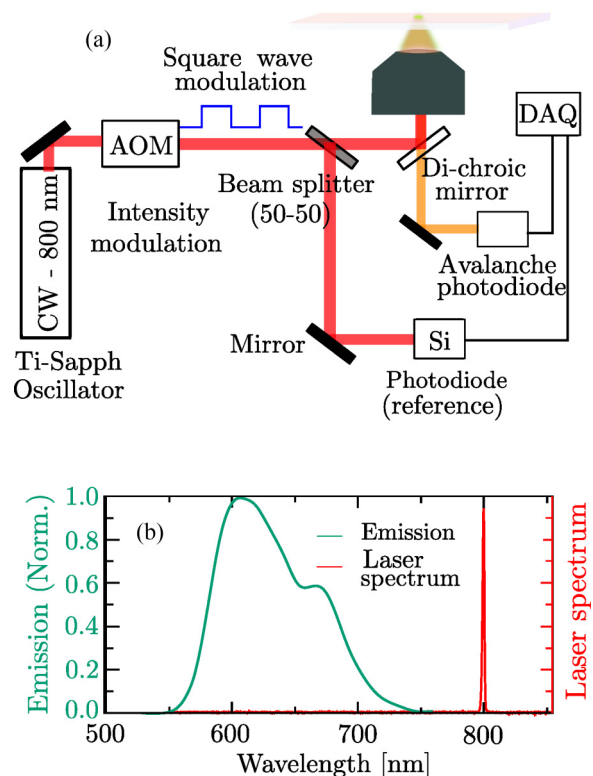


FIG. 2. (a) Schematic of the optical setup. The intensity of a beam from a CW Ti-Sapphire oscillator is modulated by an acousto-optic modulator (AOM). A beam splitter produces two beams: one for the reference (detected by a silicon photodiode) and the other to excite the sample. The emission is separated from the excitation beam using a dichroic mirror and detected by an avalanche photodiode. The signal from the avalanche photodiode is recorded by a data acquisition system (DAQ). (b) A representative spectrum of emission from the rubrene powder and the spectrum of the excitation laser.

oscillator with the output wavelength (λ_{ex}) at 800 nm is used as the light source. The laser beam passes through an acousto-optic modulator (AOM). The AOM is driven by a square wave RF signal. This modulates the intensity of the diffracted beam at the same frequency as the RF signal. A 50:50 beam splitter splits the output of the AOM into two identical replicas, one of which is detected by a silicon photodiode as a reference and the other is directed to a microscope. A reflective objective is used to focus the beam onto the sample for excitation. The emission from the sample is collected using the same microscope objective. A dichroic mirror is used to separate the UC emission from the excitation beam. Two short-pass filters (OD 4) with cut off at 675 nm are used to further suppress the scattered excitation beam. The emission is detected using an avalanche photodiode (APD). The analog signal from the APD and the reference are digitized simultaneously. Algorithms of the generalized lock-in amplifier [34,35] and coherent waveform averaging [36] are used to analyze the digitized signals. A fiber coupled spectrometer is used to record the spectra of the emission. For comparison, measurements are also done using a diode laser at 400 nm. While the overall setup of these measurements are the same, the dichroic mirror before the microscope objective is replaced by a suitable long pass dichroic filter.

III. RESULTS AND DISCUSSIONS

A typical spectrum of the emission observed in the powder of rubrene under excitation at 800 nm is shown in Fig. 2(b). It is similar to the spectra reported by Liu *et al.* [19] and Cruz *et al.* [20]. As the emission is at higher energy than the excitation, it clearly results from UC.

In order to investigate the dynamics involved in the UC, we compare the kinetics of the emission under excitation with modulated UV and NIR laser beams. Figure 3(a) shows the emission as a function of time for the single photon resonant excitation at 400 nm. A square wave modulation at about 625 Hz is applied to the laser. The figure shows the modulated intensity of the laser as the reference and the intensity of the emission from rubrene as the signal. Under the UV excitation, the reference and the emission show similar modulation Fig. 3(a). This is expected as the emission decays rapidly following a resonant excitation. Previous experiments have shown a decrease in the amplitude by three orders of magnitude within the first microseconds of impulsive excitation [37] even though the fission of the singlet excitons is extremely efficient [38]. The modulation of the emission under the NIR excitation, on the other hand, is distinctly different from that of the reference Fig. 3(b). The emission is shown for the excitation intensity of $I = 3.16 \times 10^{17}$ photons/(cm² s). The emission rises at a slower rate before reaching the steady state after about 70 μ s as shown in Fig. 3(b).

Next, we compare the measured kinetics of the emission with the simulations using the proposed models of UC in rubrene. The models proposed by Liu *et al.* [19] and Cruz *et al.* [20] uses four electronic states, S_0 , S_1 , I_m and T_1 [Fig. 1(b)]. The intermediate state is either assumed to be a virtual state [19] or a weakly resonant state [20]. In the model with weakly resonant I_m , the excitation sequentially transfers the population from S_0 to I_m and then to S_1 .

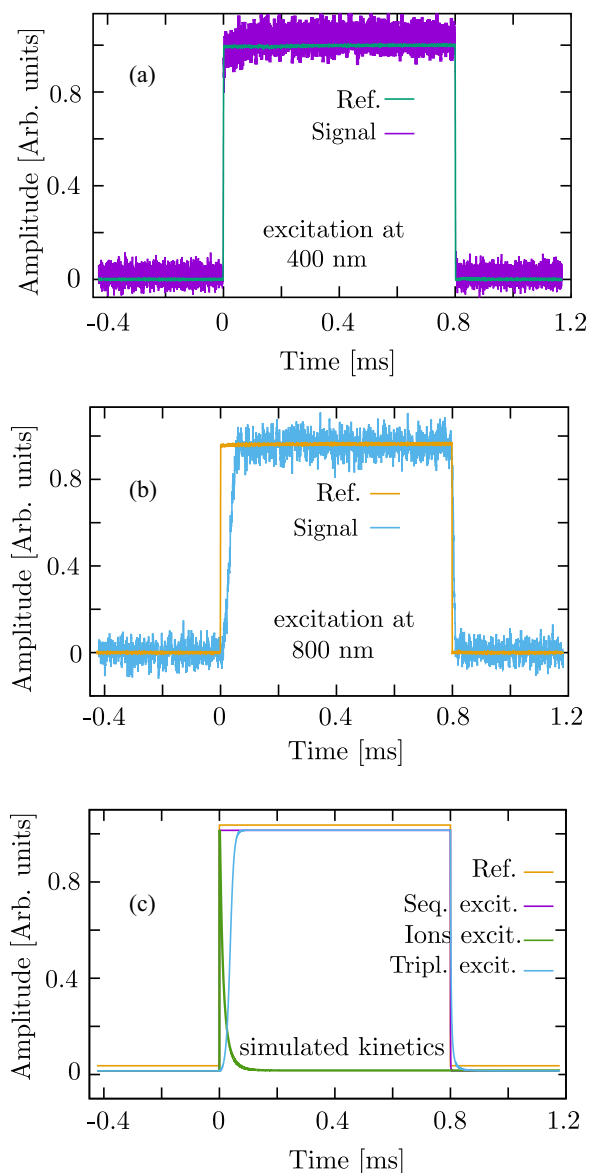


FIG. 3. Kinetics of emission under modulated excitation using (a) UV and (b) NIR laser. Simulations of the kinetics using different models (c). In (c), the reference is shifted up for clarity.

Singlet fission and TTA transfer populations between S_1 and T_1 . The kinetics simulated based on this model is shown in Fig. 3(c) and labeled as Seq. excit. The parameters of the model are absorption cross section of the intermediate state, $\sigma_{0i} = 2 \times 10^{-18}$ cm², absorption cross of intermediate state to the excited state, $\sigma_{i2} = 100 \times \sigma_{0i}$, rate of relaxation from S_1 to S_0 , $k_{10} = 6.25 \times 10^7$ s⁻¹, relaxation of the triplet, $k_{\text{trip}} = 1.67 \times 10^4$ s⁻¹, rate of fission of S_1 , $k_{\text{fiss}} = 5 \times 10^{10}$ s⁻¹, relaxation of the intermediate state, $k_i = 6.7 \times 10^5$ s⁻¹, rate of triplet-triplet annihilation, $k_{\text{TF}} = 5.4 \times 10^{-12}$ cm³s⁻¹, and self quenching rate of triplets, $k_{\text{TQ}} = 10^{-10}$ cm³s⁻¹. In this model, the number of molecules that are active in S_0 to S_i transition is 1.44×10^{19} molecules/cm³, which is about two orders of magnitude smaller than the actual density of molecules. The values are taken from the literature [20] and all the simulations whose results given in the figure are done at

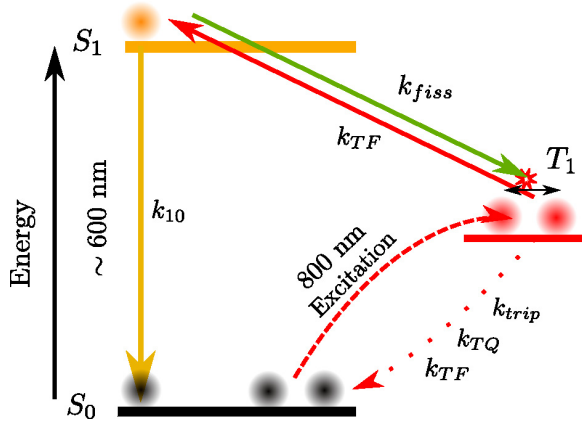


FIG. 4. Three state model used to simulate slow build up of UC emission in rubrene.

the excitation intensity that match the experimental conditions in Fig. 3(b). The kinetics simulated from this model is similar to that of the emission under UV excitation (a). It has a fast rise time. The rise time depends on the excitation density. If we lower the absorption cross section of the intermediate state by about two orders of magnitude then it matches the experimental results. However, such low absorption cross sections and low density of active molecules produce excitation densities that are similar to the ones obtained from the S_0 to T_1 transition.

The model by Beimborn *et al.* [21] is more extended. It is supported by the evidence of charged ions in the UC excitation spectra and assumes presence of ions trapped in the crystals (or microcrystals) that can be excited by the absorption of the NIR photons. The excited ions can diffuse around and when the oppositely charged ions occasionally meet, they fuse to form the triplet excitons that undergo TTA to populate the singlet excitons in S_1 . Relaxation of these excitons to S_0 results in the UC emission. The simulated kinetics of the emission from this process is shown by the green curve in Fig. 3(c), labeled as Ions. excit.). In the simulation, the rate constants k_{10} , k_{TF} , k_{TQ} , k_{trip} and k_{fiss} are taken from Ref. [20]. The density of charged species are $1.44 \times 10^{19} \text{ cm}^{-3}$ and their absorption cross-sections are $\sigma_{cs} = 10^{-16} \text{ cm}^2$. The curve shows a fast rise that is similar to the model by Cruz *et al.*, but it also decays rapidly even when the excitation is present. The decay of the emission after reaching the maximum is due to the continual depletion of the ions with excitation. The rise, as well as the decay of the signal in this model depend on the density of the trapped ions. At densities that are about eight orders of magnitude smaller than assumed in the work of Beimborn *et al.* [21], the kinetics are similar to the experimental results. Similarly, the decay becomes negligible if the absorption cross sections of the ions are reduced by six orders of magnitude. However, at such low cross sections one cannot neglect the contributions from the direct S_0 to T_1 transitions.

The limiting cases of both the models indicates that the UC emission involves initial excitation of the triplets. We use a simple three state model to explain the experimental observation (Fig. 4). We assume that the triplet excitons are excited by $S_0 \rightarrow T_1$ with a very low absorption cross section,

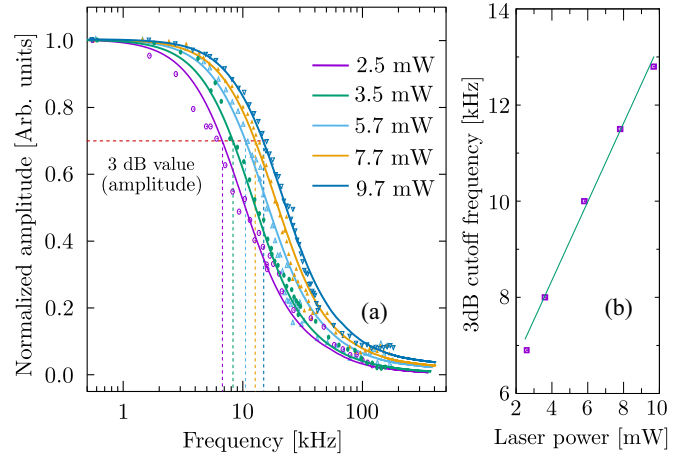


FIG. 5. The Fourier transforms of the kinetics of UC in rubrene at different excitation density. The bandwidth of the response increases with the excitation as expected from a three state model (a). The 3dB frequency is shown in (b) for the different excitations.

$\sigma_{0T} \sim 10^{-23} \text{ cm}^2$. This is about seven orders of magnitude lower than the typical cross-section for $S_0 \rightarrow S_1$ transition. Although, σ_{0T} has not been determined, most previous works have assumed it to be lower than 10^{-21} cm^2 [20]. The rate equations are given in Eqs. (2)–(4):

$$\frac{dN_{S_0}}{dt} = -\sigma_{0T}IN_{S_0} + k_{trip}N_{T_1} + (k_{TF} + k_{TQ})N_{T_1}^2 + (k_{10} - k_{fiss})N_{S_1}, \quad (2)$$

$$\frac{dN_{T_1}}{dt} = \sigma_{0T}IN_{S_0} - k_{trip}N_{T_1} - (2k_{TF} + k_{TQ})N_{T_1}^2 + 2k_{fiss}N_{S_1}, \quad (3)$$

$$\frac{dN_{S_1}}{dt} = k_{TF}N_{T_1}^2 - (k_{10} + k_{fiss})N_{S_1}, \quad (4)$$

where N_{S_0} , N_{T_1} , and N_{S_1} are the population densities in the ground state S_0 , triplet state T_1 and excited singlet state S_1 , respectively, and I is the excitation intensity. The density of molecules in the ground state is $1.434 \times 10^{21} \text{ molecules/cm}^3$. Values for the other parameters, k_{TF} , [39] k_{TQ} , [20] k_{10} and k_{fiss} [40–42] are from previous literature.

The kinetics of the emission obtained from the model is shown by blue line (labeled by Tripl. excit.) in Fig. 3(c). Although the model is simpler and depicts a pathway that has been previously suggested in anthracene [43] and tetracene, [44] it explains slow rise in the UC emission that closely match with the experiments. In this model, the lag in the emission is because the population of S_1 by TTA is efficient only when the density of the triplet excitons is high. The population of the triplets builds up during this lag time. According to this model, one expects that increase in the excitation intensity results in faster rise time, which can be easily measured in these experiments.

Therefore, we have carried out further measurements of the kinetics by varying the excitation intensity. The Fourier transforms of the kinetics are shown in Fig. 5(a). The data are analyzed in frequency domain mainly to reduce the uncertainties introduced by the large noise in the time domain

data as can be seen in Fig. 3(b). The measurements show that the bandwidth of the response function increases with the intensity. This corresponds to faster rise to the steady emission. The data from the experiments (shown by points) fit closely with the results of the simulations (shown by the lines). The dotted lines in the figure indicate the positions of the 3-dB cut-off frequency. As shown in Fig. 3(b), the cut-off frequency increases from 6 to 18 kHz for the excitation power ranging from 2.5 to 9.7 mW. The faster rise in the steady emission at higher excitation power is a clear feature of a density dependent dynamics that results from the TTA of directly excited triplets. Thus, our measurements show that TTA controls the dynamics of UC during the initial rise of the emission.

It has been noted in the previous literature that the three state model does not reproduce all the results of UC in rubrene. Particularly, it has been argued that the excitation spectrum reported by Beimborn *et al.* [21] and intensity dependence reported by Cruz *et al.*, [20] require the presence of resonant intermediate states, either formed due to charged centers (anions and cations) or defects. However, such states have not been directly observed in the absorption spectrum. This raises an interesting question: Are the intermediate states formed dynamically? For example, charges can be trapped after the UC is initiated due to the absorption by the triplets. This increases the efficiency of UC by adding new pathways for absorption. The dynamic formation of new excitation pathways implies change in the absorption crosssection, which could be measured experimentally. However, the expected cross

sections are rather small, in the range of $10^{-21} - 10^{-22} \text{ cm}^{-2}$, and their accurate measurements require significantly improved sensitivity. Nevertheless, the absorption measurements are important because they provide valuable information in explaining the UC in rubrene and also help us to understand if such processes are present more generally in other organic semiconductors such as anthracene and tetracene.

IV. CONCLUSION

To summarize, we have investigated the kinetics of UC in rubrene by using intensity modulated laser beams. Our measurements show that the emission due to UC lags the excitation and the lag time shortens with the excitation intensity. From both the observations, we conclude that the initial excitation is driven by the singlet to triplet transition ($S_0 \rightarrow T_1$). While our measurements do not exclude the previous interpretations of the process that involve resonant intermediate state, such states could be formed dynamically once the UC has initiated. Further experiments, particularly highly sensitive absorption measurements, would be necessary to conclusively prove that such intermediate states enhance UC in rubrene.

ACKNOWLEDGMENTS

This work was supported by Swedish Research Council (VR) under Grant No. 2015-05618, The World Academy of Science (TWAS) under Grant No. 20-278 RG/PHYS/AS_G-FR3240314165, and Guangdong Technion Israel Institute of Technology startup fund.

-
- [1] C. A. Parker and C. G. Hatchard, Sensitized anti-Stokes delayed fluorescence, *Proc. Chem. Soc. London* **1962**, 386 (1962).
 - [2] C. A. Parker and C. G. Hatchard, Delayed fluorescence from solutions of anthracene and phenanthrene, *Proc. R. Soc. Lond. A* **269**, 574 (1962).
 - [3] F. Deng, J. Blumhoff, and F. N. Castellano, Annihilation limit of a visible-to-uv photon upconversion composition ascertained from transient absorption kinetics, *J. Phys. Chem. A* **117**, 4412 (2013).
 - [4] T. Gatti, L. Brambilla, M. Tommasini, F. Villafiorita-Monteone, C. Botta, V. Sarritzu, A. Mura, G. Bongiovanni, and M. D. Zoppo, Near IR to red up-conversion in tetracene/pentacene host/guest cocrystals enhanced by energy transfer from host to guest, *J. Phys. Chem. C* **119**, 17495 (2015).
 - [5] T. W. Schmidt and F. N. Castellano, Photochemical upconversion: The primacy of kinetics, *J. Phys. Chem. Lett.* **5**, 4062 (2014).
 - [6] T. F. Schulze and T. W. Schmidt, Photochemical upconversion: Present status and prospects for its application to solar energy conversion, *Energy Environ. Sci.* **8**, 103 (2015).
 - [7] J. Zhou, Q. Liu, W. Feng, Y. Sun, and F. Li, Upconversion luminescent materials: Advances and applications, *Chem. Rev.* **115**, 395 (2015).
 - [8] W. Zhao and F. N. Castellano, Upconverted emission from pyrene and di-tert-butylpyrene using ir(ppy)₃ as triplet sensitizer, *J. Phys. Chem. A* **110**, 11440 (2006).
 - [9] T. N. Singh-Rachford, A. Nayak, M. L. Muro-Small, S. Goeb, M. J. Therien, and F. N. Castellano, Supermolecular-chromophore-sensitized near-infrared-to-visible photon upconversion, *J. Am. Chem. Soc.* **132**, 14203 (2010).
 - [10] R. Scheps, Upconversion laser processes, *Prog. Quantum. Electron.* **20**, 271 (1996).
 - [11] F. Auzel, Upconversion and anti-Stokes processes with f and d ions in solids, *Chem. Rev.* **104**, 139 (2004).
 - [12] D. R. Gamelin and H. U. Gudel, Upconversion processes in transition metal and rare earth metal systems, in *Transition Metal and Rare Earth Compounds. Topics in Current Chemistry.*, edited by H. Yershin (Springer, Berlin, Heidelberg, 2001), Vol. 214.
 - [13] D. K. Chatterjee, M. K. Gnanasammandhan, and Y. Zhang, Small upconverting fluorescent nanoparticles for biomedical applications, *Small* **6**, 2781 (2010).
 - [14] F. Wang, D. Banerjee, Y. Liu, X. Chen, and X. Liu, Upconversion nanoparticles in biological labeling, imaging, and therapy, *Analyst* **135**, 1839 (2010).
 - [15] J. Zhou, Z. Liu, and F. Li, Upconversion nanophosphors for small-animal imaging, *Chem. Soc. Rev.* **41**, 1323 (2012).
 - [16] T. N. Singh-Rachford and F. N. Castellano, Photon upconversion based on sensitized triplet-triplet annihilation, *Coord. Chem. Rev.* **254**, 2560 (2010), 18th International Symposium on the Photochemistry and Photophysics of Coordination Compounds Sapporo, 2009.

- [17] P. Ceroni, Energy up-conversion by low-power excitation: New applications of an old concept, *Chem. Eur. J.* **17**, 9560 (2011).
- [18] T. Schmidt and M. Tayebjee, 1.24 - upconversion, in *Comprehensive Renewable Energy*, edited by A. Sayigh (Elsevier, Oxford, 2012), pp. 533–548.
- [19] H. Liu, F. Yan, W. Li, C.-S. Lee, B. Chu, Y. Chen, X. Li, L. Han, Z. Su, J. Zhu, X. Kong, L. Zhang, and Y. Luo, Up-conversion luminescence of crystalline rubrene without any sensitizers, *Org. Electron.* **11**, 946 (2010).
- [20] C. D. Cruz, H. H. Choi, V. Podzorov, E. L. Chronister, and C. J. Bardeen, Photon upconversion in crystalline rubrene: Resonant enhancement by an interband state, *J. Phys. Chem. C* **122**, 17632 (2018).
- [21] J. C. Beimborn, W. Zagorec-Marks, and J. M. Weber, Spectroscopy of resonant intermediate states for triplet-triplet annihilation upconversion in crystalline rubrene: Radical ions as sensitizers, *J. Phys. Chem. Lett.* **11**, 7212 (2020).
- [22] X. Qian, T. Wang, and D. Yan, High mobility organic thin-film transistors based on p-p heterojunction buffer layer, *Appl. Phys. Lett.* **103**, 173512 (2013).
- [23] J. Takeya, M. Yamagishi, Y. Tominari, R. Hirahara, Y. Nakazawa, T. Nishikawa, T. Kawase, T. Shimoda, and S. Ogawa, Very high-mobility organic single-crystal transistors with in-crystal conduction channels, *Appl. Phys. Lett.* **90**, 102120 (2007).
- [24] V. C. Sundar, J. Zaumseil, V. Podzorov, E. Menard, R. L. Willett, T. Someya, M. E. Gershenson, and J. A. Rogers, Elastomeric transistor stamps: Reversible probing of charge transport in organic crystals, *Science* **303**, 1644 (2004).
- [25] M. J. Currie, J. K. Mapel, T. D. Heidel, S. Goffri, and M. A. Baldo, High-efficiency organic solar concentrators for photovoltaics, *Science* **321**, 226 (2008).
- [26] V. Podzorov, E. Menard, A. Borissov, V. Kiryukhin, J. A. Rogers, and M. E. Gershenson, Intrinsic Charge Transport on the Surface of Organic Semiconductors, *Phys. Rev. Lett.* **93**, 086602 (2004).
- [27] S. Tao, N. Ohtani, R. Uchida, T. Miyamoto, Y. Matsui, H. Yada, H. Uemura, H. Matsuzaki, T. Uemura, J. Takeya, and H. Okamoto, Relaxation Dynamics of Photoexcited Excitons in Rubrene Single Crystals using Femtosecond Absorption Spectroscopy, *Phys. Rev. Lett.* **109**, 097403 (2012).
- [28] G. B. Piland, J. J. Burdett, D. Kurunthu, and C. J. Bardeen, Magnetic field effects on singlet fission and fluorescence decay dynamics in amorphous rubrene, *J. Phys. Chem. C* **117**, 1224 (2013).
- [29] K. J. Karki, L. Kringle, A. H. Marcus, and T. Pullerits, Phase-synchronous detection of coherent and incoherent nonlinear signals, *J. Opt.* **18**, 015504 (2015).
- [30] K. J. Karki, Increasing the density of modes in an optical frequency comb by cascaded four-wave mixing in a nonlinear optical fiber, *Phys. Rev. A* **96**, 043802 (2017).
- [31] J. Chen, A. Krasavin, P. Ginzburg, A. V. Zayats, T. Pullerits, and K. J. Karki, Evidence of high-order nonlinearities in supercontinuum white-light generation from a gold nanofilm, *ACS Photonics* **5**, 1927 (2018).
- [32] P. Kumar and K. J. Karki, Two-photon excitation spectroscopy of 1,5-diphenyl-1,3,5-hexatriene using phase modulation, *J. Phys. Commun.* **3**, 035008 (2019).
- [33] P. Kumar, Q. Shi, and K. J. Karki, Enhanced radiative recombination of excitons and free charges due to local deformations in the band structure of MAPbBr₃ perovskite crystals, *J. Phys. Chem. C* **123**, 13444 (2019).
- [34] K. J. Karki, M. Torbjörnsson, J. R. Widom, A. H. Marcus, and T. Pullerits, Digital cavities and their potential applications, *J. Instrum.* **8**, T05005 (2013).
- [35] S. Fu, A. Sakurai, L. Liu, F. Edman, T. Pullerits, V. Öwall, and K. J. Karki, Generalized lock-in amplifier for precision measurement of high frequency signals, *Rev. Sci. Instrum.* **84** (2013).
- [36] M. Olsson, F. Edman, and K. J. Karki, Direct measurement of fast transients by using boot-strapped waveform averaging, *Rev. Sci. Instrum.* **89**, 035104 (2018).
- [37] A. Rysanyanskiy and I. Biaggio, Triplet exciton dynamics in rubrene single crystals, *Phys. Rev. B* **84**, 193203 (2011).
- [38] I. Biaggio and P. Irkhin, Extremely efficient exciton fission and fusion and its dominant contribution to the photoluminescence yield in rubrene single crystals, *Appl. Phys. Lett.* **103**, 263301 (2013).
- [39] K. A. Ward, B. R. Richman, and I. Biaggio, Nanosecond pump and probe observation of bimolecular exciton effects in rubrene single crystals, *Appl. Phys. Lett.* **106**, 223302 (2015).
- [40] Y. Ishibashi, Y. Inoue, and T. Asahi, The excitation intensity dependence of singlet fission dynamics of a rubrene microcrystal studied by femtosecond transient microspectroscopy, *Photochem. Photobiol. Sci.* **15**, 1304 (2016).
- [41] L. Ma, K. Zhang, C. Kloc, H. Sun, M. E. Michel-Beyerle, and G. G. Gurzadyan, Singlet fission in rubrene single crystal: Direct observation by femtosecond pump-probe spectroscopy, *Phys. Chem. Chem. Phys.* **14**, 8307 (2012).
- [42] K. Miyata, Y. Kurashige, K. Watanabe, T. Sugimoto, S. Takahashi, S. Tanaka, J. Takeya, T. Yanai, and Y. Matsumoto, Coherent singlet fission activated by symmetry breaking, *Nat. Chem.* **9**, 983 (2017).
- [43] H. Port and D. Rund, Temperature dependent triplet absorption spectra of anthracene crystals. photoexcitation spectroscopy with a dye-laser, *Chem. Phys. Lett.* **54**, 474 (1978).
- [44] G. Vaubel and H. Baessler, Delayed fluorescence and triplet lifetime in tetracene crystals, *Phys. Status Solidi B* **37**, K31 (1970).